CHEMISTRY OF MATERIALS
Article

Chem. Mater. **2010,** *22,* 4295–4303 4295
DOI:10.1021/cm1011229

Traditional and Microwave-Assisted Solvothermal Synthesis and Surface Modification of Co_7 Brucite Disk Clusters and Their Magnetic Properties

Yan-Ling Zhou,[†] Ming-Hua Zeng,*[,†] Lian-Qiang Wei,[†] Bin-Wen Li,[†] and Mohamedally Kurmoo*[,‡]

[†]*Key Laboratory of Synthetic and Natural Functional Molecule Chemistry of the Ministry of Education, Northwest University, Xi'an 710069, P R China, School of Chemistry and Chemical Engineering, Guangxi Normal University, Guilin 541004, P R China, and* [‡]*Laboratoire DECOMET, CNRS-UMR 7177, Université de Strasbourg, 4 rue Blaise Pascal, 67000 Strasbourg Cedex, France*

Received April 22, 2010. Revised Manuscript Received June 7, 2010

We present the comparative preparation of $[Co_7(\mu_3\text{-}OH)_6(L)_6](ClO_4)_2 \cdot 12H_2O$ (**1**), $[Co_7(\mu_3\text{-}CH_3O)_6(L)_6](ClO_4)_2$ (**2**), and $[Co_7(\mu_3\text{-}N_3)_6(L)_6](ClO_4)_2$ (**3**), where HL is 2-methoxy-6-[(methylimino)-methyl]phenol, using traditional (e.g., 120 °C, 120 h, 23% yield for **1**) and microwave-assisted (e.g., 120 °C, 10 min, 46% yield for **1**) solvothermal synthesis. The structures contain Co_7 brucite disk $[Co_7(\mu_3\text{-}X)_6(\mu_2\text{-}O)_6]^{2+}$, where the ligands are arranged in two open hemispheres and the flat inner surface is functionalized when X is OH^-, CH_3O^-, and N_3^-. The symmetry of the core decreases in the order **1** > **2** > **3**, according to the shape, size, and rigidity of the inner bridges (X). These units are stacked into a chain, and for **1**, the water molecules provide a hydrogen-bonded network through the hydroxyl groups. Interestingly, electrospray ionization mass spectrometry (ESI-MS) indicates that the heptacobalt(II) clusters of **1**−**3** exist in solution and the their compositions in solution are similar to those in the solid. However, the inner ligands μ_3-CH_3O^- and N_3^- are replaced partially with μ_3-OH^-, indicating that μ_3-OH^- has a greater affinity than μ_3-CH_3O^- or N_3^- for Co^{II}, and the parental core of $[Co_7(OH)_6(L)_6]^{2+}$ is the most stable of the three compounds in solution. The presence of edge-sharing octahedra through μ_3-O or μ_3-N provides ferromagnetic coupling between nearest neighbors in all cases. Interestingly, for μ_3-N, it appears to be stronger than μ_3-O which resulted in single-molecule magnet (SMM) behavior at a higher temperature of 3 K, while they are below the limit of the SQUID magnetometers (2 K) in the case of **1** and **2**.

Introduction

In the past decade, much attention has been devoted to the design and synthesis of the magnetic polymetallic cluster since the discovery of "single-molecule magnets" (SMMs).[1−3] Many methods for controlling the structure and magnetism of these clusters have been pursued.[3,4] In fact, an important factor in the construction of such clusters is the choice of the "key" ligand, which will dictate not only the symmetry, topology, and number of paramagnetic metal ions but also the intramolecular and intermolecular interactions of the clusters.[5,6] From the point of view of organic ligand design, it is desirable to synthesize bulky ligands that have the coordinating atoms pointing on one side of the molecule, this favoring magnetic isolation of the clusters,[7] and also mainly changing the correlation of the magnetic clusters.[8] On the other hand, the short bridges have extreme versatile bridging abilities in linking neighboring metal ions (μ_2, μ_3, μ_4, etc.), thus strengthening the stability, and also are the key to acquiring predictable magnetic exchange along with the cooperation of appropriate external ligands.[3,9] Unfortunately, structurally related clusters for subtly

*To whom correspondence should be addressed. E-mail: zmh@mailbox.gxnu.edu.cn (M.-H.Z.) or kurmoo@unistra.fr (M.K.).

(1) Fujita, M., Powell, A., Creutz, C., Eds. *From the molecular to the nanoscale: Synthesis, structure, and properties*; Elsevier Ltd.: Oxford, U.K., 2004; Vol. *7*.
(2) (a) Gatteschi, D.; Sessoli, R.; Villain, J. *Molecular Nanomagnets*; Oxford University Press: Oxford, U.K., 2006. (b) Gatteschi, D.; Sessoli, R. *Angew. Chem., Int. Ed.* **2003**, *42*, 268. (c) Stamatatos, T. C.; Christou, G. *Inorg. Chem.* **2009**, *48*, 3308.
(3) (a) Zeng, M.-H.; Yao, M.-X.; Liang, H.; Zhang, W.-X.; Chen, X.-M. *Angew. Chem., Int. Ed.* **2007**, *46*, 1832. (b) Chen, Q.; Zeng, M.-H.; Zhou, Y.-L.; Zou, H.-H.; Kurmoo, M. *Chem. Mater.* **2010**, *22*, 2114.
(4) (a) Christou, G. *Polyhedron* **2005**, *24*, 2065. (b) Feng, P. L.; Koo, C.; Henderson, J. J.; Manning, P.; Nakano, M.; Barco, E. D.; Hill, S.; Hendrickson, D. N. *Inorg. Chem.* **2009**, *48*, 3480.
(5) Inglis, R.; Jones, L. F.; Milios, C. J.; Datta, S.; Collins, A.; Parsons, S.; Wernsdorfer, W.; Hill, S.; Spyros, P. P.; Piligkos, S.; Brechin, E. K. *Dalton Trans.* **2009**, 3403.
(6) (a) Yang, E.-C.; Wernsdorfer, W.; Zakharov, L. N.; Karaki, Y.; Yamaguchi, A.; Isidro, R. M.; Lu, G.-D.; Wilson, S. A.; Rheingold, A. L.; Ishimoto, H.; Hendrickson, D. N. *Inorg. Chem.* **2006**, *45*, 529. (b) Feng, P. L.; Koo, C.; Henderson, J. J.; Nakano, M.; Hill, S.; Barco, E.; Hendrickson, D. N. *Inorg. Chem.* **2008**, *47*, 8610.
(7) (a) Li, B.-W.; Zhou, Y.-L.; Chen, Q.; Zeng, M.-H. *Polyhedron* **2010**, *29*, 148. (b) Zhou, Y.-L.; Meng, F.-Y.; Zhang, J.; Zeng, M.-H.; Liang, H. *Cryst. Growth Des.* **2009**, *9*, 1402.
(8) (a) Zaleski, C. M.; Depperman, E. C.; Dendrinou-Samara, C.; Alexiou, M.; Kampf, J. W.; Kessissoglou, D. P.; Kirk, M. L.; Pecoraro, V. L. *J. Am. Chem. Soc.* **2005**, *127*, 12862. (b) Miyasaka, H.; Yamashita, M. *Dalton Trans.* **2007**, 399.
(9) Wang, X.-Y.; Wang, Z.-M.; Gao, S. *Chem. Commun.* **2008**, 281.

Published on Web 06/24/2010

Table 1. Basal Summary of Co_7 Brucite Disk Clusters

compound[a]	Co···Co (Å)[b]	μ_3-X bridges	∠Co−X−Co (deg) (μ_3-X)	∠Co−X′−Co (deg) (μ-X′)[c]	magnetic behavior[d]
$[Co^{III}Co^{II}_6(thme)_2(O_2CCMe_3)_8Br_2]\cdot MeCN$[11]	3.094	-OR	95.19−101.18	106.82	F
$[Co^{II}_3Co^{III}_4(hep)_6(MeO)_6]$[12]	3.093	-OR	89.376−101.53	103.91	F
$[Co^{II}_4Co^{III}_3(dea)_6(Ac)_3](ClO_4)_{0.75}(Ac)_{1.25}\cdot 0.5H_2O$[13]	3.085	-OR	94.41−97.87	106.80	F
$[Co^{II}_4Co^{III}_3(ea)_6(NO_3)_3(H_2O)_3][NO_3]_2\cdot 9MeOH\cdot 4.5H_2O$[14]	3.063	-OR	95.27−97.65	105.17	F (SMM)
$[Co^{II}_7(bzp)_6(N_3)_9(CH_3O)_3]\cdot 2ClO_4\cdot 2H_2O$[15]	3.185	-OMe, -N_3	93.24−95.26	99.07	F (SMM)
$[Co^{II}_7(hdeo)_6(N_3)_6]\cdot(ClO_4)_2\cdot 2H_2O$[16]	3.274	-N_3	96.16−98.55	107.48	F (SMM)
$[Co^{II}_7(CH_3O)_6(immp)_6](ClO_4)_2$[17]	3.158	-OMe	95.40−99.04	102.85	F
$[Co^{II}_7(OH)_6(L)_6](ClO_4)_2\cdot 12H_2O$ (this work)	3.099	-OH	96.35−98.58	102.57	F
$[Co^{II}_7(CH_3O)_6(L)_6](ClO_4)_2$ (this work)	3.141	-OMe	94.41−98.21	102.69	F
$[Co^{II}_7(N_3)_6(L)_6](ClO_4)_2$ (this work)	3.174	-N_3	94.94−98.75	104.21	F (SMM)

[a] hep is 1,1,1-trifluoro-7-hydroxy-4-methyl-5-azahept-3-en-2-one. H_2dea is diethanolamine. Hhdeo is 2-hydroxy-[1,2-di(pyridin-2-yl)]ethan-1-one. H_3ea is $H_2NC(CH_2OH)_3$. bzp is 2-benzoylpyridine. immp is 2-iminomethyl-6-methoxyphenolic anion. [b] The mean Co···Co distances within the core of clusters. [c] The mean Co−μ-X′−Co angles within the core of clusters. [d] F indicates ferromagnetic exchange.

modulating the effect of short bridges (such as OH^-/CH_3O^-/N_3^-)[10] exist, though detailed comparison of structure−property relationships is still lacking.

Disklike heptacobalt clusters were discovered some time ago and have seven Co^{II} and (or) Co^{III} ions; six inner μ_3 and six outer μ_2 short bridges are alternately aligned in the disk.[11−17] Even if the inner bridged group size and its hardness vary, the Co_7 disks can "breathe" over a small range to accommodate this (Table 1). Thus, there are four common inner bridges within heptanuclear complexes: (i) six μ_3-OR,[11−14] (ii) three μ_3-N_3 and μ_3-MeO,[15] (iii) six μ_3-N_3,[16] and (iv) six μ_3-MeO[17] bridged Co^{II} or mixed Co^{II} and Co^{III} disks have been reported. Almost all the disks have a high-spin ground state because the magnetic orbitals of Co^{II} and (or) Co^{III} are accidentally orthogonal. Three of these disks show SMM behavior because magnetic anisotropy of Co^{II} can be controlled by a change in the coordination geometries of the Co^{II} ions.[14−16] Hence, disklike Co_7 cluster systems offer an advantage for achieving such chemical control, through the substitution of various bridging and bulky ligands into a given structure type. Furthermore, the nature of the magnetic exchange coupling between different bridging ligand in the resulting cluster is readily predicted.

In our previous study, a disklike and ferromagnetic heptanuclear cluster was synthesized by the microwave-assisted method, $[Co_7(CH_3O)_6(immp)_6](ClO_4)_2$ (immp is 2-iminomethyl-6-methoxyphenolic anion),[17] where classical intermolecular N−H/O hydrogen bonds are constructed by N−H groups of immp ligands and ClO_4^- anions. In this work, analogous anion L = 2-methoxy-6-[(methylimino)methyl]phenol

Scheme 1. Formation of Compounds 1−3

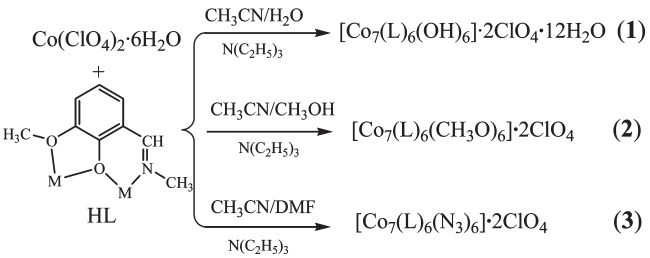

was introduced, acting as peripheral ligand and favoring magnetic isolation of the clusters. Under suitable solvents and additional ligand, the reactions afford three "inner bridge (μ_3-OH/CH_3O/N_3) switchings" of disk Co^{II}_7 complexes (Scheme 1 and Figure 1). Both dc and ac magnetization data suggest a significant difference in their magnetic behaviors. This observation raises an interesting question regarding its origin and provides a remarkable model for the modulated effect of inner bridges in molecular clusters. Furthermore, an evaluation of the microwave-assisted solvothermal reaction in comparison to the traditional one has been provided, providing evidence of the greater effectiveness over time, and of the quality and quantity of materials. On the other hand, ESI-MS is becoming a powerful technique in the discovery of the complexity of cluster-based coordination systems in solution.[19] Interestingly, our ESI-MS experiments indicate that the heptacobalt(II) clusters of **1**−**3** exist in solution and their compositions in solution are similar to those in the solid and also reveal that subtle substitutions of the CH_3O^-, N_3^- core bridges by OH^- occur for **2** and **3**.

Experimental Section

Materials and Physical Measurements. All chemicals were commercially available and used as received without further purification. Microwave synthesis was conducted using a WX-4000 microwave digestion system. Elemental analyses (CHN) were performed using an Elemental Vario-EL CHN elemental analyzer. FT-IR spectra were recorded from KBr pellets in the range of 4000−400 cm^{-1} on a Bio-Rad FTS-7 spectrophotometer. To confirm the phase purity of the bulk materials, X-ray powder diffraction (XRPD) experiments were conducted with all prepared samples of **1**−**3**. The powder XRPD data were collected on a Rigaku D/max 2200 diffractometer with Cu Kα radiation. The XRPD experimental and simulated patterns are shown in Figure S1

(10) Klöwer, F.; Lan, Y.; Nehrkorn, J.; Waldmann, O.; Anson, C. E.; Powell, A. K. *Chem.—Eur. J.* **2009**, *15*, 7413.
(11) Moragues-Canovás, M.; Talbot-Eeckelaers, C. E.; Catala, L.; Lloret, F.; Wernsdorfer, W.; Brechin, E. K.; Mallah, T. *Inorg. Chem.* **2006**, *45*, 7038.
(12) Chibotaru, F. L.; Ungur, L.; Aronica, C.; Elmoll, H.; Pilet, G.; Luneau, D. *J. Am. Chem. Soc.* **2008**, *130*, 12445.
(13) Tudor, V.; Marin, G.; Lloret, F.; Kravtsove, V. C.; Simonov, Y. A.; Julve, M.; Andruh, M. *Inorg. Chim. Acta* **2008**, *361*, 3446.
(14) Ferguson, A.; Parkin, A.; Sanchez-Benitez, J.; Kamenev, K.; Wernsdorfer, W.; Murrie, M. *Chem. Commun.* **2007**, 3473.
(15) Zhang, Y.-Z.; Wernsdorfer, W.; Pan, F.; Wang, Z.-H.; Gao, S. *Chem. Commun.* **2006**, 3302.
(16) Wang, X.-T.; Wang, B.-W.; Wang, Z.-M.; Zhang, W.; Gao, S. *Inorg. Chim. Acta* **2008**, *361*, 3895.
(17) Zhan, S.-H.; Song, Y.; Liang, H.; Zeng, M.-H. *CrystEngComm* **2009**, *11*, 865.

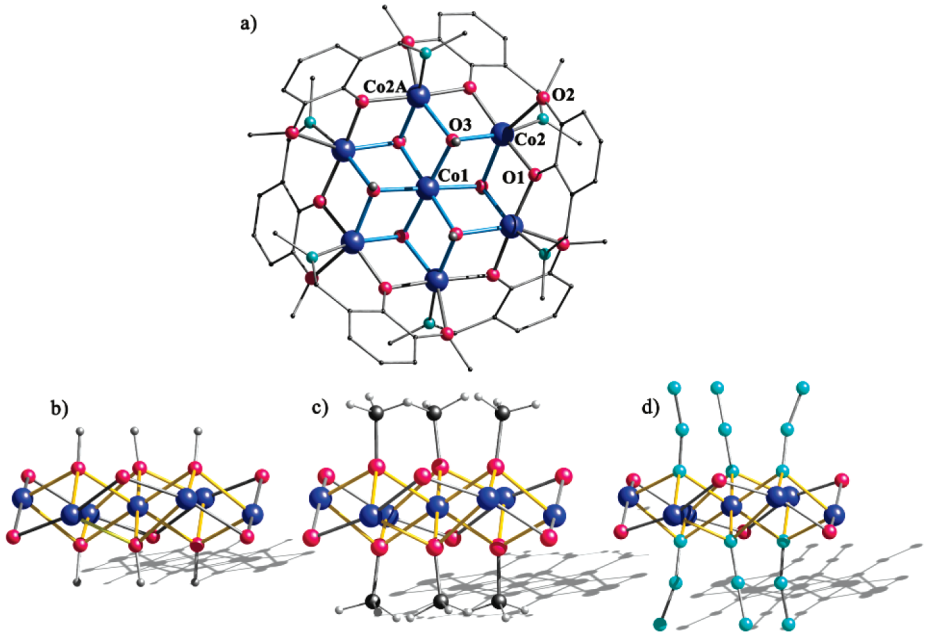

Figure 1. (a) Molecular structure of **1** and core structures of **1** (b), **2** (c), and **3** (d). Organic H atoms and ClO_4^- have been omitted for the sake of clarity.

of the Supporting Information. The experimental patterns of compounds **1**−**3** are in good agreement with the corresponding simulated ones, confirming the phase purity of the as-synthesized products. The ESI mass spectra were recorded using an HCT mass spectrometer (Bruker Daltonics) under conditions in which the needle and capillary exit voltages were set to 4 kV and 200 V, respectively; the desolvation chamber temperature was set to 573 K. Magnetization measurements were taken with a Quantum Design MPMS-XL5 SQUID to 5 T for **1**−**3**. Data were corrected for the diamagnetism of the gelatin sample holder and the constituent atoms using Pascal's constants.

Synthesis. The ligand 2-methoxy-6-[(methylimino)methyl]phenol (HL) was prepared according to the literature procedure.[17] **Caution:** Azide and perchlorate complexes of metal ions are potentially explosive. Only a small amount of material should be prepared, and it should be handled with caution.

$[Co_7(L)_6(OH)_6](ClO_4)_2 \cdot 12H_2O$ (*1*). (*i*) *Microwave Method.* A solution of $Co(ClO_4)_2 \cdot 6H_2O$ (0.360 g, 1 mmol), HL (0.271 g, 1 mmol), and triethylamine (0.8 mL) in 30 mL of mixed solvent (1:4 water/acetonitrile) was placed in a 60 mL Teflon-lined autoclave, which was then inserted into the cavity of a microwave reactor. The reaction mixture was maintained at 120 °C, 300 W, and 6.3 atm for a total of 10 min. After the solution had cooled (ca. 2 h), the red crystals of **1** were collected by filtration, washed with acetonitrile, and dried in air. Phase pure crystals of **1** were obtained by manual separation (yield of 154 mg, ca. 45.9% based on Co). Elemental analyses calcd for **1** ($Co_7C_{54}H_{90}N_6O_{38}Cl_2$): C, 33.87%; H, 4.74%; N, 4.39%. Found: C, 33.80%; H, 4.78%; N, 4.35%. IR data for **1** (KBr, cm^{-1}): 3443(s), 2930(w), 1638(s), 1560(w), 1481(s), 1463(s), 1322(m), 1221(s), 1120(s), 1092(s), 967(w), 865(s), 746(m), 625(w), 485(w).

(*ii*) *Traditional Method.* HL (0.271 g, 1 mmol) was added to the solution of $Co(ClO_4)_2 \cdot 6H_2O$ (0.360 g, 1 mmol) in the mixed solvent (1:4 water/acetonitrile) (7 mL). The mixture was stirred for 15 min, and then 0.8 mL of triethylamine was added. The mixture was placed in a 15 mL Teflon-lined stainless steel autoclave and heated at 120 °C for 120 h. The autoclave was cooled over a period of 8 h at a rate of 10 °C/h. The red crystals of **1** were collected by filtration, washed with methanol, and dried in air. Phase pure crystals of **1** were obtained by manual separation (yield of 77.5 mg, ca. 23.1% based on Co). IR spectroscopy and XRPD confirmed this product to be complex **1**.

$[Co_7(L)_6(CH_3O)_6] \cdot 2ClO_4$ (*2*). Complex **2** was prepared by a procedure similar to that employed for complex **1**, except that the 1:4 methanol/acetonitrile mixed solvent was used instead of the 1:4 water/acetonitrile mixed solvent.

(*i*) *Microwave Method.* Yield of 144.6 mg, ca. 43.1% based on Co. Elemental analyses calcd for **2** ($Co_7C_{60}H_{78}N_6O_{26}Cl_2$): C, 33.87%; H, 4.74%; N, 4.39. Found: C, 33.82%; H, 4.81%; N, 4.32%. IR data for **2** (KBr, cm^{-1}): 3444(s), 2933(w), 1637(s), 1562(w), 1459(s), 1312(s), 1223(s), 1078(s), 965(m), 860(w), 746(s), 624(m), 484(m).

(*ii*) *Traditional Method.* Yield of 45.6 mg, ca. 13.6% based on Co. IR spectroscopy and XRPD confirmed this product to be complex **2**.

$[Co_7(L)_6(N_3)_6] \cdot 2ClO_4$ (*3*). Complex **3** was prepared by a procedure similar to that employed for complex **1** in the presence of NaN_3, and the 1:4 methanol/acetonitrile mixed solvent was replaced with the 1:4 DMF/acetonitrile mixed solvent.

(*i*) *Microwave Method.* Yield of 138.9 mg, ca. 41.4% based on Co. Elemental analyses calcd for **1** ($Co_7C_{54}H_{60}N_{24}O_{20}Cl_2$): C, 35.08%; H, 3.27%; N, 18.18%. Found: C, 33.12%; H, 3.78%; N, 18.35%. IR data for **1** (KBr, cm^{-1}): 3419(m), 2934(w), 2082(s), 1634(s), 1460(s), 1406(w), 1241(m), 1220(s), 1097(s), 963(w), 793(w), 749(s), 624(s), 484(m).

(*ii*) *Traditional Method.* Yield of 37.9 mg, ca. 11.3% based on Co. IR spectroscopy and XRPD confirmed this product to be complex **3**.

Crystal Structure Determination. Single-crystal X-ray diffraction data collection for the three compounds was conducted on a Bruker SMART APEX CCD diffractometer equipped with graphite monochromated Mo Kα radiation (λ = 0.71073 Å) by using the $\theta-\omega$ scan technique at 123 K. Raw frame data were integrated using SAINT. The structures were determined by direct methods with SHELXS-97 and refined by full-matrix least-squares on F^2 using SHELXS-97.[18] Empirical absorption

(18) (a) Sheldrick, G. M. *SHELXTL*, version 6.14; Bruker AXS Inc.: Madison, WI, 2003. (b) Sheldrick, G. M. *SADABS* (*the Siemens Area Detector Absorption Correction*); University of Göttingen: Göttingen, Germany, 1996.

Table 2. Crystal Data and Structure Refinement for 1−3

	1	2	3
formula	$Co_7C_{54}H_{90}N_6O_{38}Cl_2$	$Co_7C_{60}H_{78}N_6O_{26}Cl_2$	$Co_7C_{54}H_{60}N_{24}O_{20}Cl_2$
Fw	1914.73	1782.69	1848.64
crystal system	trigonal	trigonal	trigonal
space group	*P*-3*c*1	*P*-3*c*1	*P*-3*c*1
T (K)	173(2)	173(2)	173(2)
a (Å)	14.045(8)	14.230(1)	14.1074(8)
b (Å)	14.045(8)	14.230(1)	14.1074(8)
c (Å)	23.235(3)	23.544(3)	23.882(3)
α (deg)	90.00	90.00	90.00
β (deg)	90.00	90.00	90.00
γ (deg)	120.00	120.00	120.00
V (Å^3)	3969.0(5)	4128.5(4)	4116.2(6)
D_c (g/cm^3)	1.602	1.434	1.492
Z	2	2	2
μ (mm^{-1})	1.585	1.429	1.516
no. of reflections collected	17751	11669	15322
no. of idependent reflections	7453	6127	5821
goodness of fit on F^2	1.029	1.042	1.141
$R_1{}^a$ [$I > 2\sigma(I)$]	0.0561	0.0709	0.0771
$wR_2{}^b$ (all data)	0.2868	0.1869	0.2361
largest difference peak and hole (e/Å^3)	−0.714/1.963	−0.812/1.757	−0.712/1.856

$^aR_1 = \sum||F_o| - |F_c||/\sum|F_o|$. $^b wR_2 = [\sum w(F_o{}^2 - F_c{}^2)^2/\sum w(F_o{}^2)^2]^{1/2}$.

correction was applied using SADABS.[18] All non-hydrogen atoms were refined anisotropically. The hydrogen atoms were set in calculated positions and refined using the riding model. The anisotropic displacement parameters of atoms (O6, C10, C13, and C14) in **1** and **2** were restrained to be identical with a standard uncertainty of 0.01 Å for terminal atoms. The crystallographic details are provided in Table 1, while the selected bond distances and angles are listed in Tables 2 and 3, respectively, for **1**−**3**. Crystallographic data for the structural analyses have been deposited at the Cambridge Crystallographic Data Center. CCDC reference numbers are 773827−773829 for **1**−**3**, respectively.

Results and Discussion

Synthetic Aspects. There are three main points about the syntheses of these compounds. One is the technique used, the second the solvent in relation to the final product, and the third the time of the reaction. In the case of **1** and **2** (Figure 2), we find that the microwave-assisted solvothermal synthesis gave the better results in terms of yield and also in the quality of crystals (size, morphology, and optical clarity).[17,20] The yield and the size of the crystals increase with the time of the reaction in the microwave process. For **3**, the yield is low and the microwave technique is performed better. However, the crystal size remains small (Figure 3 and Figure S2 of the Supporting Information).

The solvent plays an important role in the synthesis as it defines the pressure inside the reactors and, most importantly, is involved in the reactions. In the presence of a mixture of water and acetonitrile under slightly basic conditions, the hydroxide is the favored coordinating ligand in the μ_3 position. When the water is replaced with methanol, the methoxide replaces the hydroxide in the crystals, and in the absence of water and methanol but with DMF in place and additional azide, the latter is the favored coordinating ligand.

Compounds **2** and **3** are stable in air under ambient conditions. However, crystals of **1** can be directly isolated from the solution but will rapidly lose crystallinity as soon as they are removed from their mother liquor, indicating a loss of the solvent molecules. The three compounds are soluble in water, acetonitrile, and DMF, and this character suggests we can explore their electronic spectra to investigate the short bridge stabilities.

Crystal Structures of 1−3, $[Co_7(L)_6(\mu_3\text{-}X)_6](ClO_4)_2$. The three compounds crystallize in trigonal space group *P*-3*c*1, and each consists of the cationic heptanuclear cluster (Figure 1). Disregarding the small differences in the inner μ_3-X ligands, we find that the central cores of **1**−**3** are essentially isostructural, and their selected interatomic distances and angles are compared in Table 2.

The structures of complexes **1**−**3** contain two counteranions ClO_4^-, a cationic cluster $[Co_7(L)_6(\mu_3\text{-}X)_6]^{2+}$ [X is OH (**1**), OCH_3 (**2**), or N_3 (**3**)] and solvent water in **1**. The seven Co^{II} centers are essentially coplanar (Figure 1) as expected for all edge-sharing octahedra and can be considered as a segment of the brucite $Mg(OH)_2$ layer and thus a symmetric disk. The Co_7 units are held together by six μ_3-X and six O atoms of six $\eta^1{:}\eta^2{:}\eta^1{:}\mu_2$ bridging organic L ligands. The six μ_3-X ligands bridge the Co_6 hexagon with the central Co atom with three on each surface and the six μ_2-O bridging Co_2 pairs at the periphery of the hexagon. Six N atoms and six O atoms from the corresponding L ligand complete the peripheral ligation around the metallic core. The six L ligands are arranged as two open hemispheres with a common back and ligand X sitting in the bowl. In **1**−**3**, the average coordination bond lengths involving the μ_2-O1 atoms are 1.994, 2.019, and 2.023 Å and the μ_3-O3 atom (in **1** and **2**) or μ_3-N2 atom (in **3**) bond lengths are in the ranges of 2.027−2.067, 2.028−2.109, and 2.066−2.192 Å, respectively (Table 3). The bridging angles of the Co−O1−Co bonds, which determine the sign of the magnetic exchange interactions through oxygen bridges, are 102.57°, 102.69°, and 104.22°, respectively, and the bridging angles of the Co−X−Co bonds are in the ranges of 96.46−98.69°, 94.41−98.22°, and 94.53−98.34°, respectively (Figure 4). Hence, the mean Co···Co distances within the clusters increase smoothly in the sequence **1** < **2** < **3** (mean values of 3.099, 3.141, and 3.174 Å, respectively), which we can probably assign to the combined effects of the different μ_3-bridging ligands. The different coordination environments are due to the steric strain on the Co^{II} ions, and the small difference reflects the structural difference between **2** or **3** and **1** in that the inner exchange is OH^-, which likely imposes the highest conjugated disklike plane for **1** based on structural symmetry. The differences in the

(19) (a) Lin, X.; Doble, D. M. J.; Blake, A. J.; Harrison, A.; Wilson, C.; Schröder, M. *J. Am. Chem. Soc.* **2003**, *125*, 9476. (b) Bai, Y.-L.; Tao, J.; Huang, R.-B.; Zheng, L.-S. *Angew. Chem., Int. Ed.* **2008**, *47*, 5344. (c) Miras, H. N.; Wilson, E. F.; Cronin, L. *Chem. Commun.* **2009**, 1297 and references cited therein . (d) Cooper, G. J. T.; Newton, G. N.; Long, D.-L.; Kögerler, P.; Rosnes, M. H.; Keller, M.; Cronin, L. *Inorg. Chem.* **2009**, *48*, 1097.

(20) Zhang, S.-H.; Zhou, Y.-L.; Sun, X.-J.; Wei, L.-Q.; Zeng, M.-H.; Liang, H. *J. Solid State Chem.* **2009**, *182*, 2991.

Table 3. Metal−Ligand Bond Lengths (angstroms) and Angles (degrees) in Compounds 1−3[a]

compound **1**		compound **2**		compound **3**	
Co1−O3	2.067(1)	Co1−O3	2.109(3)	Co1−N2	2.107(5)
Co2−O1	2.009(2)	Co2−O1	2.029(4)	Co2−O1	2.039(5)
Co2−O1A	1.978(1)	Co2−O1A	2.009(4)	Co2−O1A	2.006(5)
Co2−O2	2.346(2)	Co2−O2	2.329(5)	Co2−O2	2.301(6)
Co2−O3	2.073(1)	Co2−O3	2.028(4)	Co2−N2	2.066(5)
Co2−O3A	2.027(2)	Co2−O3A	2.068(4)	Co2−N2A	2.192(5)
Co2−N1	2.048(2)	Co2−N1	2.105(6)	Co2−N1	2.081(6)
Co1···Co2	3.088(1)	Co1···Co2	3.128(2)	Co1···Co2	3.156(2)
Co2···Co2A	3.110(2)	Co2···Co2A	3.154(2)	Co2···Co2A	3.192(3)
Co2−O1−Co2A	102.57(6)	Co2−O1−Co2A	102.69(2)	Co2−O1−Co2A	104.22(2)
Co1−O3−Co2	96.46(6)	Co1−O3−Co2	94.41(1)	Co1−N2−Co2	94.53(2)
Co1−O3−Co2A	97.91(6)	Co1−O3−Co2A	97.96(4)	Co1−N2−Co2A	97.17(2)
Co2−O3−Co2A	98.69(5)	Co2−O3−Co2A	98.22(2)	Co2−N2−Co2A	98.34(2)
O3−Co1−O3A	97.98(3)	O3−Co1−O3A	97.13(1)	N2−Co1−N2A	96.45(5)
O1−Co2−O1A	166.7(1)	O1−Co2−O1A	165.6(1)	O1−Co2−O1A	162.95(1)

[a]Symmetry code: $x - y$, x, $-z + 1$.

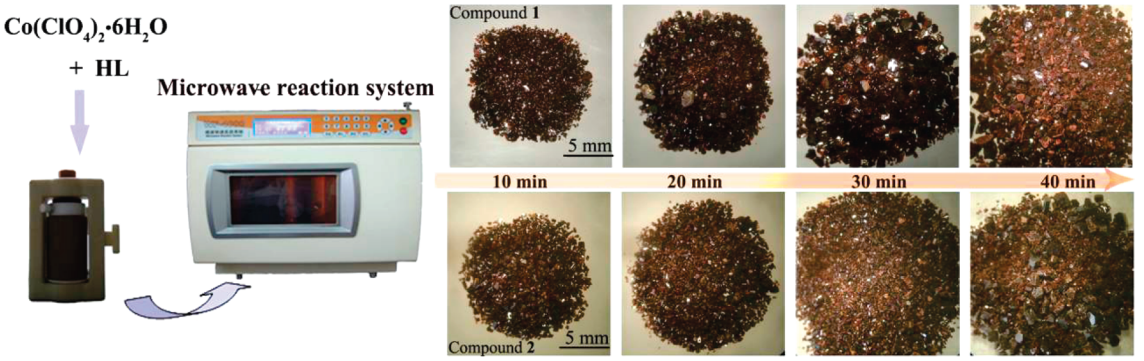

Figure 2. Series of optical microscope images of single crystals for compounds **1** (top) and **2** (bottom) with different reaction times by microwave-assisted synthesis.

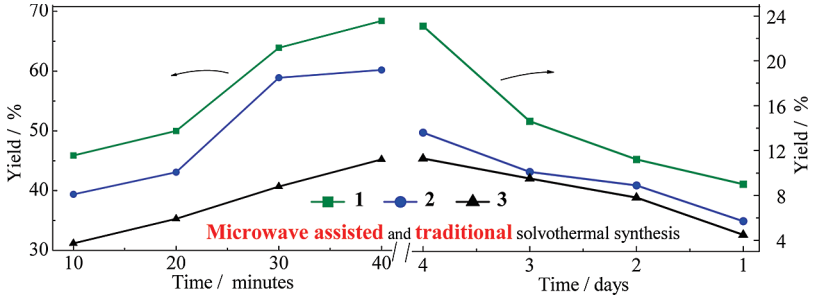

Figure 3. Comparison of the formation of compounds **1**−**3** under microwave-assisted (MW) and traditional solvothermal (TS) conditions for different periods of time.

bond length and angle modes lead to the different behaviors in solution stability and their magnetic susceptibility data. The three compounds mentioned above are reminiscent of $[Co_7(bzp)_6(N_3)_9(CH_3O)_3](ClO_4)_2 \cdot 2H_2O$ reported by Gao et al.[15] mixed bridged by 3/4 azides and 1/4 methoxide. It is of note that the structural motif belongs to the recently reported disklike $\{Co_7\}$ family. Although there are a number of disklike Co_7 complexes now known, complexes **1**−**3** provide the first examples in which the μ_3-X ligand can chemically be replaced without much change to the rest of the structure.[11−17]

The disklike Co_7 units for **1**−**3** are well isolated by bulky L and ClO_4^-, without intermolecular hydrogen bonds and the nearest intercluster center−center distances of 14.04, 14.23, and 14.11 Å, respectively, in the

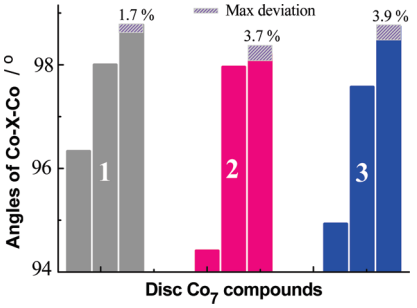

Figure 4. Co−X−Co bridging angles for bonds of compounds **1**−**3**.

a−b plane (Figure 5). The nearest intercluster Co−Co distances are 11.62, 11.77, and 11.94 Å, respectively, in the c direction, and compounds **2** and **3** have bigger bulky

inner bridging groups and a smaller void space for any solvent molecule to fit in the *c* direction, when compared to **1**. Therefore, no packing solvate or water molecules are found in the crystal lattice of compounds **2** and **3**. Hence, intermolecular interactions between the metal complex and lattice solvate molecules are not an issue in the two compounds. Recently, it was reported that the lattice solvate molecule has a profound influence on the QTM in Mn_4 SMMs.[21] The absence of lattice solvent molecules in compounds **2** and **3** makes them relatively "clean" candidates for the study of QTM. However, the molecules in the crystal lattice of compound **1** pack upon each other in an offset fashion forming sheets with the "free" volume and the H_2O solvent molecules occupying the space between Co_7 complexes along the *c* direction. In other words, docking of the free volume molecule within the cavity of the bowl-shaped cluster of **1** (Figure 6). It is interesting that all the water molecules are linked by 12 hydrogen bonds, affording a (H_2O) cluster with an adamantoid structure. Adjacent O···O distances lie in the range of 2.65−2.94 Å, with an average of 2.795 Å, and bond angles are in the range of 104.1−154.6°, with an average value of 113.1°. The distance across the heptanuclear is 14.62 Å, and these clusters are further linked with neighboring heptanuclear complex moieties by sextruple hydrogen bonds with the inner bridging OH ligand, forming a chainlike structure along the *c* axis. For these hydrogen bonds, the O···O distance is 3.31 Å and the bond angle is 137.5°.

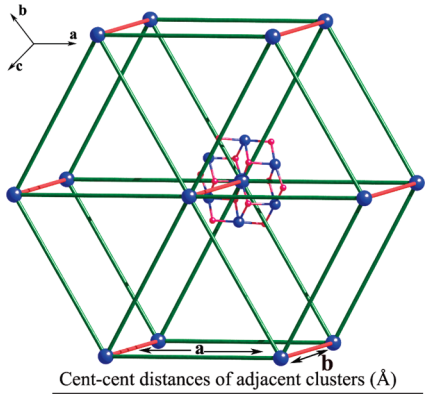

Cent-cent distances of adjacent clusters (Å)

	1	2	3
a	14.04	14.23	14.11
b	11.62	11.77	11.94

Figure 5. Illustrative view of the links between clusters from one Co^{II}_7 center.

ESI-MS Spectroscopic Properties. Characterization of the clusters in solution was accomplished by ESI-MS experiments which give further evidence of different exchange processes of the inner bridging group within the heptanuclear units. For the acetonitrile solution of **1**−**3**, the ESI mass spectrum of **1** (Figure 7) exhibits the main ion peaks observed at a mass of 749.53 as a result of losing all solvent molecules, two ClO_4^- to form $[Co_7(OH)_6(L)_6]$. The weak singly charged ion peak (*m*/*z* 1597.95) can be assigned as $\{[Co_7(OH)_9(L)_6]ClO_4\}_2$. The ESI mass spectrum of **2** is different from that of **1** (Figure 8), and the spectral peaks associated with doubly charged states of $[Co_7(CH_3O)_2(OH)_4(L)_6]$, $[Co_7(CH_3O)_3(OH)_3(L)_6]$, $[Co_7(CH_3O)_4(OH)_2(L)_6]$, $[Co_7(CH_3O)_5(OH)(L)_6]$, and $[Co_7(CH_3O)_6(L)_6]$ segments were found at *m*/*z* 763.50, 770.50, 777.56, 784.56, and 791.56, respectively. In other words, the inner CH_3O^- bridges are replaced step by step by OH^-. The ESI mass spectrum of **3** shows characteristics similar to those of **2** (Figure 9), and the doubly charged ion peaks at *m*/*z* 774.50, 787.06, and 799.50 can be assigned to $[Co_7(N_3)_2(OH)_4(L)_6]$, $[Co_7(N_3)_3(OH)_3(L)_6]$, and $[Co_7(N_3)_4(OH)_2(L)_6]$, respectively. The observed masses clearly matched the assigned formulas as well as the simulated spectra. Interestingly, changing the core voltage used to obtain positive ion ESI mass spectra of solutions of **2** and **3** did not significantly alter their appearance (Figure S4 and S5 of the Supporting Information). This suggests that compounds **2** and **3** produced in solution were stable during the ionization process. Hence, these data support the same conclusion as the electronic spectroscopic study, namely that inner bridge μ_3-OH is the most stable and has greater affinity than μ_3-CH_3O and N_3 for Co^{II} ions, and the stability of the disklike compounds decreases in the order **1** > **2** > **3**.

Why is the -OH inner bridged compound **1** the most stable in solution? Usually, the stabilities of the clusters described above are mainly determined by the affinity of the inner bridges for seven Co^{II} ions, whereby the μ-O outer bridges from the bulky peripheral ligand link together six Co^{II} ions. The shape and size of the singly negatively charged inner bridges OH^-, CH_3O^-, and N_3^-

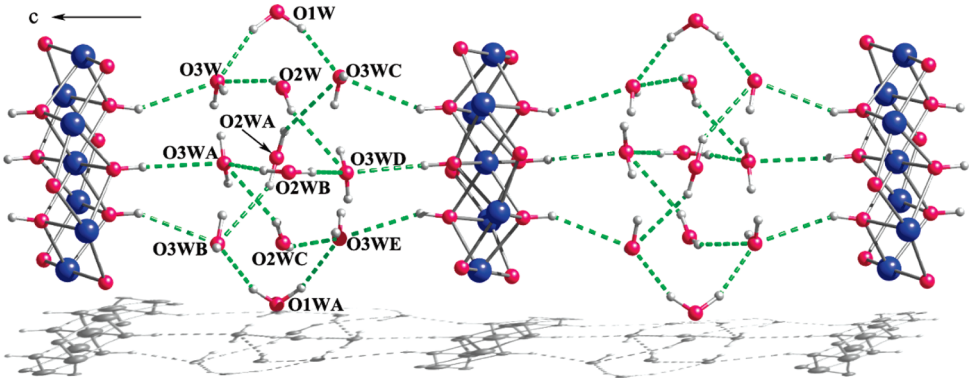

Figure 6. View of a one-dimensional chain linked by intermolecular hydrogen bonds between $(H_2O)_{12}$ clusters and OH^- bridging ligands in **1**. Some hydrogen atoms and L ligands have been omitted for the sake of clarity.

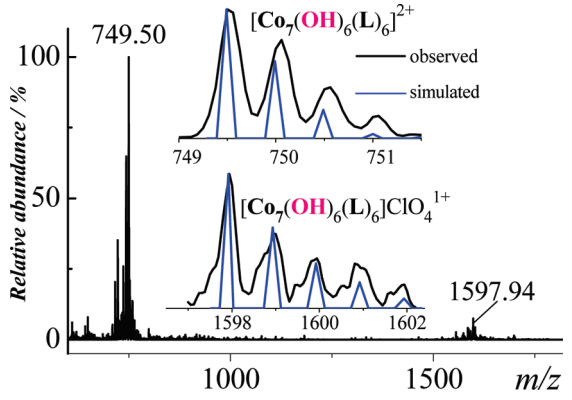

Figure 7. ESI mass spectrum of **1** in acetonitrile. The black lines show the experimental data, and the blue lines are simulations of the isotope pattern.

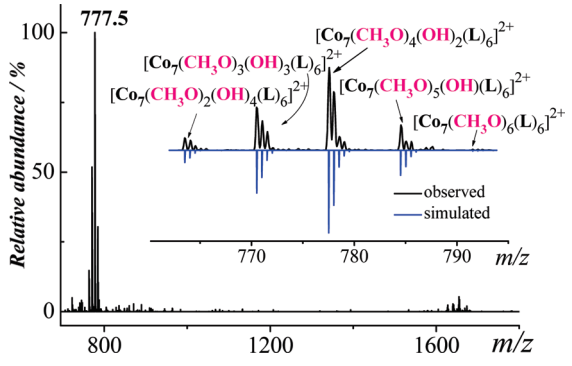

Figure 8. ESI mass spectrum of **2** in acetonitrile. The black line shows the experimental data, and the blue line is a simulation of the isotope pattern.

define the stability of the whole Co_7 clusters. Thus, the small and linear OH^- bridges promote the formation of the highest symmetry (smallest deviation for Co−O bond distances and Co−X−Co angles) as seen in **1**. However, the bigger bulky CH_3O^- and N_3^- bridge three Co^{II} ions of lower symmetry in **2** and **3** (Figure 4), respectively. On the other hand, the OH groups interact more covalently with Co^{II} ions because of the decrease in "hardness" in the order $OH^- > CH_3O^- > N_3^-$. Hence, μ_3-OCH_3/N_3 inner bridges in **2** and **3** can be replaced by μ_3-OH in the presence of traces of water,[22] together with the corresponding fragmentation products. The inner bridge μ_3-OH is the most stable and has greater affinity than μ_3-CH_3O/N_3 for Co^{II} ions, while μ_3-N_3 is least stable in solution, thus leading to the absence of the $[Co_7(N_3)_6(L)_6]^{2+}$ fragmentation. Hence, **1** shows greater solution stability than compounds **2** and **3**. ESI-MS studies helped us not only to identify and establish the integrity of the cluster but also to observe the different short bridge effects in stabilizing the cluster core. This case offers a new example for the limited ESI-MS studies, which also have been successfully utilized to provide the information for understanding the assembly of clusters. To the best of our knowledge, it is the first time ESI-MS has

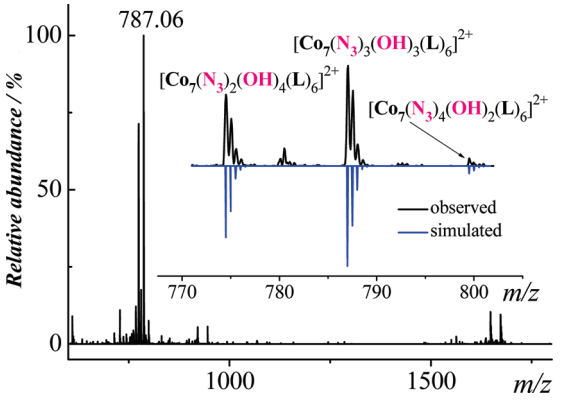

Figure 9. ESI mass spectrum of **3** in acetonitrile. The black line shows experimental data, and the blue line is a simulation of the isotope pattern.

been successfully utilized to examine such a series of inner bridge replacement reactions for Co_7-based clusters, complementing the work of Cronin et al.[23] on supramolecular cluster transformation ($Co_{12} \rightarrow Co_{13}$) by ESI-MS.

Magnetic Properties. *Direct Current Magnetic Susceptibility Studies*. Magnetic studies were performed with crushed single-crystal samples of **1**−**3** in an applied field of 1 kOe in the temperature range of 1.8−300 K. To facilitate comparison of the three Co_7 clusters with different inner bridging ligands, the molar susceptibility data were calculated by using a heptanuclear formula weight. The obtained data for **1**−**3** are plotted in Figure 10 as $\chi_m T$ versus T. The $\chi_m T$ products of **1**−**3** overlap almost completely in the high-temperature regime and diverge only below ca. 50 K, indicating similar paramagnetic behavior at high temperatures but slightly different magnetic behavior at low temperatures. For each of the samples, the value of $\chi_m T$ at 300 K is ~20 $cm^3\ mol^{-1}\ K$, which is much higher than the spin-only value of seven high-spin Co(II) ions (13.1 $cm^3\ mol^{-1}\ K$), indicating significant orbital contributions of the octahedral Co(II) ions.[3,24] The reciprocal molar magnetic susceptibility plotted versus temperature of the three compounds obeys the Curie−Weiss law above 50 K with a C of 19.84 emu K mol^{-1} and a θ of 1.16 K for **1**, a C of 19.80 emu K mol^{-1} and a θ of 0.74 K for **2**, and a C of 19.48 emu K mol^{-1} and a θ of 1.88 K for **3**. The positive Weiss constants suggest that the dominant intracluster coupling is ferromagnetic. When the temperature is < 50 K, the $\chi_m T$ values of the three complexes increase continuously at different rates, reaching maxima of 37, 29.6, and 30 $cm^3\ mol^{-1}\ K$ for **1**−**3**, respectively, below 10 K. The slight difference in behavior may be associated with the effect of the X ligands, which indicate a stronger coupling constant for the azide as also found for the Weiss constant. Interestingly, only **3** displays a rounded maximum at 3 K.

We investigated the variation of the magnetization M with the applied magnetic field H for **1**−**3** in the range 0−5 T at 2 K (Figure 11). The field dependence of M shows a rapid increase with H, confirming the overall

(21) Wernsdorfer, W.; Aliaga-Alcalde, N.; Hendrickson, D. N.; Christou, G. *Nature* **2002**, *416*, 406.
(22) Aromí, G.; Ribas, J.; Gamez, P.; Roubeau, O.; Kooijman, H.; Spek, A. L.; Teat, S.; MacLean, E.; Stoeckli-Evans, H.; Reedijk, J. *Chem.—Eur. J.* **2004**, *10*, 6476.
(23) Newton, G. N.; Cooper, G. J. T.; Kögerler, P.; Long, D.-L.; Cronin, L. *J. Am. Chem. Soc.* **2008**, *130*, 790.
(24) Kurmoo, M. *Chem. Soc. Rev.* **2009**, *38*, 1353.

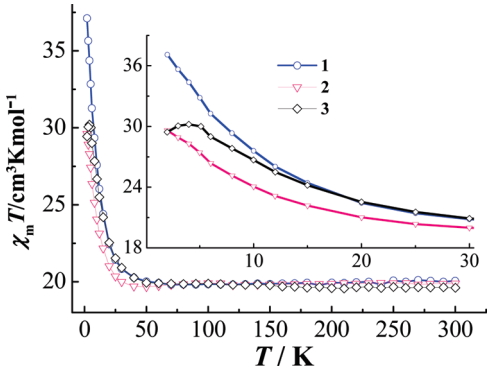

Figure 10. Plot of $\chi_m T$ vs T for **1**−**3** in the temperature range of 2−300 K. The inset is a plot of $\chi_m T$ vs T for **1**−**3** at low temperatures.

intermolecular ferromagnetic coupling. The magnetization reached 17.47, 14.65, and 10.79 Nβ for **1**−**3**, respectively, at 5 T. The value for **1** is just higher than that expected for seven paramagnetic cobalt(II) atoms of 16.8 Nβ assuming 2.4 Nβ per Co(II), while those of **2** and **3** are lower. If we assume ferromagnetic coupling leading to an effective $S_T = {}^7/_2$ spin ground state, the estimated g values are 4.99, 4.19 and 3.08, respectively. This is also consistent with the $\chi_m T$ value at low temperatures and confirms that interaction between the Co^{II} ions is ferromagnetic. This observation of ferromagnetic coupling between cobalt neighbors is consistent with the previous work on brucite layered structures.[17,24]

Alternating Current Magnetic Susceptibility Studies. As a means of investigating the magnetization relaxation dynamics, ac magnetic susceptibilities of complexes **1**−**3** were studied. The ac susceptibility measurements in zero dc field were performed in the range of 1−997 Hz. The in- and out-of-phase ac susceptibilities have no dependence on frequency between 2 and 10 K for compounds **1** and **2** (Figure S6 of the Supporting Information), but in the case of the azido compound **3**, a significant frequency dependence on the in-phase and out-of-phase ac signals (χ' and χ'') was observed below 3.5 K (Figure 12). A maximum of the χ' signal appears at 2 K under the ac frequency of 1000 Hz. Even down to the 1.9 K limit of our magnetometer, no peaks are seen in χ'', which is similar to that seen in other heptanuclear cobalt clusters, such as $[Co^{II}_4Co^{III}_3(HL)_6(NO_3)_3(H_2O)_3]$ [$H_3L = H_2NC(CH_2OH)_3$][14] and $[Co^{II}_7(bzp)_6(N_3)_9(CH_3O)]_3$.[15] The ac susceptibility measurements at lower temperatures will be needed to estimate the energy barrier to reorientation of the moments. The energy gap (D), which is related to the relaxation time (τ_0) in a SMM, can be tuned by an applied dc field. From the curve of the field dependence of the ac susceptibility of **3**, we find that the out-of-phase signal χ'' reaches the maximum at an H of 1900 Oe. Therefore, a static field of 1900 Oe was applied to measure the ac susceptibilities. As a result, both in-phase and out-of-phase signals move to higher temperatures (Figure 12). The χ' peaks were observed at ac frequencies higher than 300 Hz, different from the other heptanuclear cobalt compounds,[11−13,16,17] which confirms the larger

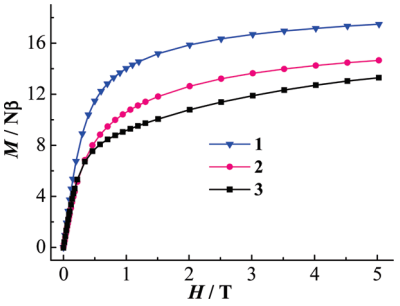

Figure 11. Field dependence of the magnetization for **1**−**3** at 2 K.

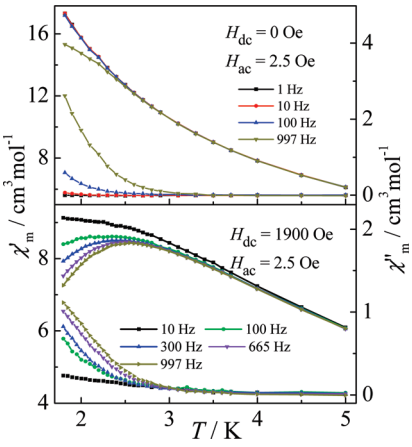

Figure 12. Temperature dependence of the real (top) and imaginary (bottom) components of the ac susceptibility in zero applied static field (up) and 1900 Oe (down) with an oscillating field of 2.5 Oe.

energy barrier of **3**. The shift of the peak temperature (T_P) of χ' is measured by a parameter $\varphi = (\Delta T_P/T_P)/\Delta(\log f) = 0.086$,[25] which is larger than that for a canonical spin glass, closer to a normal value for a superparamagnet. Slow relaxation is seen in ac magnetic susceptibility; however, only very broad steps could be observed at 1.8 K, and it was impossible to obtain suitable magnetization versus time decay data to construct a reliable Arrhenius plot. Data collected from 1 to 997 Hz at 1.8−2.3 K in applied fields of $H = 0$, which seem to show beginnings of a semicircle plot (especially at 1.8 K) (Figure S9 of the Supporting Information).[3,26]

*Influence of the Bridges on the Nature of the Magnetic Coupling in **1**−**3***. The detailed analyses of the magnetic data of **1**−**3** show that the μ-oxo (L ligand), μ_3-X double bridge provides the exchange pathway for the ferromagnetic couplings observed in three compounds. The strength of the exchange follows the sequence **3** > **1** > **2**, taking the θ values into consideration. It is expected that the μ-oxo (L ligand) with larger values for the Co−O−Co angle (102.57, 102.69, and 104.22°, respectively) would result in antiferromagnetic coupling, which is found in a large number of magneto-structural studies on oxygen atom-bridged clusters and networks. Furthermore, the biggest difference is 1.6°, found in the Co−O−Co angle, and it is expected that the strongest antiferromagnetic coupling occurs in **3**. As far as the μ_3-OH, CH_3O, N_3 bridges are

(25) Mydosh, J. A. *Spin Glasses: An Experimental Introduction*; Taylor & Francis: London, 1993.

(26) Schelter, E. J.; Prosvirin, A. V.; Dunbar, K. R. *J. Am. Chem. Soc.* **2004**, *126*, 15004.

concerned, with some "harder" OH^- than CH_3O^-, N_3^- is softest group. The reason for **3** to show significant slow relaxation at static zero field below 3 K toward SMM behavior is unclear. It is possible that the Co^{II} ions are in a less symmetrical ligand field for **3**; it has an easy-axis anisotropy and may show SMM behavior, whereas when it is in a more symmetrical environment, it has an easy-plane anisotropy and exhibits non-SMM behavior.[2b,27]

Conclusion

In summary, the combination of cobalt ions, as well as a special Schiff base ligand L, is a good strategy for obtaining disklike $Co^{II}{}_7$ systems, where the inner bridges can be changed from -OH to $-OCH_3$ and $-N_3$ using different reaction solvents, in the presence or absence of additional bridging ligands. The microwave-assisted solvothermal technique gives better quality crystals and better yield in a shorter period than the conventional one. This method can provide a new, fast, and powerful synthetic tool for acquiring new polymetallic complexes. ESI-MS provides evidence of the existence of the clusters in solution and demonstrates the exchange of the inner bridging ligands in favor of hydroxide. Hence, this work further highlights the potential role that ESI-MS can play as a rapid screening tool in ligand exchange development. Magnetic measurements show the inner bridge replacement affects the ground-state anisotropy of $Co^{II}{}_7$ clusters and, in addition, provides a simple way to tune toward single-molecule magnet (SMM) behavior. This is a rare example of how changing the identity of inner bridges can significantly change their solution stability and magnetic properties without affecting the overall topology of the complexes.

Acknowledgment. This work was supported by NSFC (20871034), NSFGX (2010GXNSFF013001), the Program for New Century Excellent Talents in University of the Ministry of Education China (NCET-07-217), the Project of Ten, Hundred, Thousand Distinguished Talents in New Century of Guangxi (2006201), the Ying Tung Education Foundation (111014), and the Université de Strasbourg and CNRS (France).

Supporting Information Available: Crystallographic data (CIF), XRD and TG measure, plot of the in-phase (χ') and out-of-phase (χ'') ac susceptibility signals for **1** and **2** and dc field dependence of the ac susceptibility of **3** at 2 K, Cole−Cole plots for **3**, and data collected from 1 to 997 Hz at 1.8−2.3 K with a zero dc field. This material is available free of charge via the Internet at http://pubs.acs.org.

(27) Gatteschil, D.; Sorace, L. *J. Solid State Chem.* **2001**, *159*, 253.